Jour. Fac. Sci., Hokkaido Univ., Ser. IV,
vol. 18, no. 3, Mar., 1978, pp.305-338.

PHASE EQUILIBRIA IN THE SYSTEM $MgSiO_3$-Al_2O_3-Fe_2O_3 AT HIGH TEMPERATURES AND PRESSURES, WITH SPECIAL REFERENCE TO THE SOLUBILITY OF Al_2O_3 AND Fe_2O_3 IN ENSTATITE

by

Makoto Arima

(with 34 text-figures and 4 tables)

(Contribution from the Department of Geology and Mineralogy,
Faculty of Science, Hokkaido University, No. 1550)

Abstract

The phase equilibria in the system $MgSiO_3$-Al_2O_3-Fe_2O_3 were determined experimentally in the temperature and pressure range 800 – 1300°C and 8 – 16 Kb. The following phase assemblages were encountered, the single phase of enstatite solid solution(ss), $enstatite_{ss}$+hematite, $enstatite_{ss}$+$sapphirine_{ss}$+quartz, $enstatite_{ss}$+$spinel_{ss}$+quartz, $enstatite_{ss}$+$spinel_{ss}$+hematite+quartz. The solubility of Al_2O_3 and Fe_2O_3 in enstatite was determined experimentally. The solubility of $MgFe^{3+}AlSiO_6$ in enstatite by the substitution $MgSi = Fe^{3+}Al$, increases with increasing temperature and decreasing pressure. It is confirmed that Al_2O_3 is incorporated in enstatite by the substitution MgSi = AlAl as well as $MgSi = Fe^{3+}Al$. The solubility of Al_2O_3 in enstatite increases with increasing Fe_2O_3 content in it at constant temperature and pressure. The solubility of $MgAl_2SiO_6$ by the substitution MgSi = AlAl, however, is constant at constant temperature and pressure, indicating the possibility of using the $MgAl_2SiO_6$ content of orthopyroxene as an indicator of temperature and/or pressure with taking mineral assemblage into account.

Mössbauer spectra measurements were made on some synthetic enstatites. Fe^{3+} preferes to enter in the octahedral site (MI) rather than the tetrahedral site (T). Small amount of tetrahedral Fe^{3+} was confirmed indicating the substitution $MgSi = Fe^{3+}Fe^{3+}$ at high temperatures.

Some geological significances of Al_2O_3 and Fe_2O_3 contents of orthopyroxenes are discussed. The present experimental results indicate that total Al_2O_3 contents of orthopyroxene can not be used as an indicator of temperature and/or pressure, but Al_2O_3 content in $MgAl_2SiO_6$ should be used.

Introduction

The solubility of Al_2O_3 in orthopyroxene is one of the important problem in experimental mineralogy and petrology, related to the stability of high aluminous orthopyroxenes occurring in ultramafic inclusion within volcanic rocks and in high grade metamorphic rocks.

Boyd and England (1964) studied the solubility of Al_2O_3 in enstatite in the pressure range 20 – 50 Kb and showed that the solubility of Al_2O_3 in

enstatite coexisting with pyrope is very sensitive to pressure variation and the Al_2O_3 content of orthopyroxene may be used as an indicator of pressure. This result was also confirmed by MacGregor and Ringwood (1964), Green and Ringwood (1967), and MacGregor (1974).

At 1 atmospheric pressure, the solubility of Al_2O_3 in protoenstatite was studied by Biggar and Clark (1973) in the system CaO-MgO-Al_2O_3-SiO_2 and Onuma and Arima (1975) in the system $MgSiO_3$-$MgAl_2SiO_6$. From these experiments, Onuma and Arima (1975) showed that only 1.75 wt.% Al_2O_3 was incorporated in protoenstatite at high temperature.

In their study on the solubility of Al_2O_3 in enstatite in the pressure range 1 – 5 Kb, Anastasiou and Seifert (1972) showed that the solubility increases with increasing temperature (9 wt.% Al_2O_3 at 1200°C even at 1 Kb) but does not strongly depend on the pressure.

The pressure dependence of the solubility of Al_2O_3 in enstatite coexisting with spinel and forsterite was also determined by MacGregor (1974), Fujii and Takahashi (1976), and Obata (1976). The experimental results by Fujii and Takahashi (1976) and the thermodynamic study by Obata (1976), however, showed only a slight pressure dependence and they suggested that the Al_2O_3 content of orthopyroxene coexisting with spinel and olivine can not be used as an indicator of pressure.

Arima and Onuma (1977) studied the phase equilibria in the system $MgSiO_3$-$MgAl_2SiO_6$ in the pressure range 10 – 25 Kb with special reference to the solubility of Al_2O_3 in enstatite. From these results, they suggested that the Al_2O_3 content of orthopyroxene can not be used either as a pressure indicator or as a temperature indicator without taking the mineral assemblage into account.

In order to elucidate the stability of high aluminous orthopyroxene, it is important to determine the effect of other cations such as Fe^{2+}, Fe^{3+}, Ca, Cr, Ti, and Na on the solubility of Al_2O_3 in enstatite. This problem has been studied experimentally by Wood (1973) on the system $MgSiO_3$-$Fe^{2+}SiO_3$-Al_2O_3, by Akella (1976) on the system $MgSiO_3$-$CaSiO_3$-Al_2O_3 with reference to the pressure estimation on spinel lherzolites or garnet lherzolites. Holdaway (1976) also investigated the system $MgSiO_3$-$Fe^{2+}SiO_3$-Al_2O_3 to determine the solubility of Al_2O_3 in orthopyroxene coexisting with cordierite.

There is, however, no experimental study on the effect of Fe^{3+} on the stability of high aluminous orthopyroxene. As shown in Fig. 1, some natural high aluminous orthopyroxenes contain also high Fe_2O_3, indicating the substitution $MgSi = Fe^{3+}Al$ in orthopyroxene. When Al_2O_3 is incorporated in orthopyroxene by both the substitution $MgSi = AlAl$ and $MgSi = Fe^{3+}Al$, the Al_2O_3 content of orthopyroxene can not be treated in the system

$(MgFe^{2+}Ca)SiO_3$-Al_2O_3. In order to elucidate the stability of high aluminous orthopyroxene, therefore, it is necessary to determine the pressure and temperature dependence of the substitution $MgSi = Fe^{3+}Al$ and its influence on the substitution $MgSi = AlAl$.

In this paper, the stability of enstatite in the system $MgSiO_3$-Al_2O_3-Fe_2O_3 and the solubility of Al_2O_3 and Fe_2O_3 in enstatite are determined experimentally in the pressure and temperature range 8 – 16 Kb and 800 – 1300°C. The geological significances of Al_2O_3 and Fe_2O_3 contents of orthopyroxenes are discussed.

Previous works

The join $MgSiO_3$-$MgAl_2SiO_6$ at 1 atm.

The join $MgSiO_3$ (En)-$MgAl_2SiO_6$ (MgATs) was studied by Onuma and

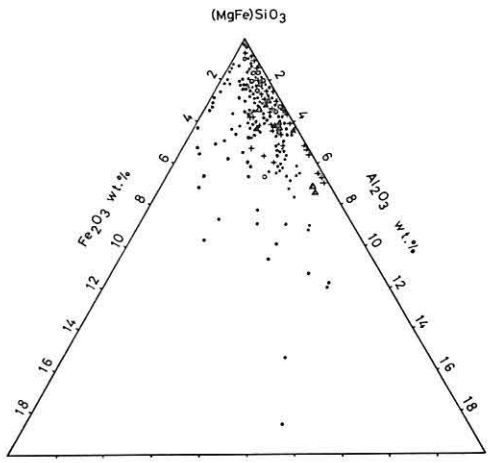

Fig. 1 Al_2O_3 and Fe_2O_3 contents of natural orthopyroxenes. Sources of data. *Plutonic differentiated rocks and volcanic rocks* (open circle) Hess (1952), Brown (1957), Kuno (1954, 1964), Atkins (1969). *Intrusive peridotite* (triangle) Green (1964), Onuki (1965), Challis (1965), Takeda and Onuki (1973), Niida (unpublished). *Inclusion of volcanic rock* (cross mark) Ross (1954), Banno (1964), Lovering (1964, 1969), Onuki (1965), Meyer (1976), Le Maitre (1965). *Metamorphic rock* (solid circle) Eskola (1952), Howie and Subramaniam (1957), O'hara (1960, 1961), Kranck (1961), Binns (1962, 1965), Dodd (1963), McKie (1963), Barker (1964), Engel et al. (1964), Green (1964), Howie (1963, 1964), Sen and Rege (1965), Klein (1966), Philpotts (1966), Leelanandam (1967), Chinner and Sweatman (1968), Davidson (1968), Bhattacharyya (1970), Bondarenko (1972), Lutts and Kopanava (1972), Nixon et al. (1973), Clifford (1975), Jayawardene and Carswell (1976), Murthy (1976), Wilson (1976), Woodford and Wilson (1976), Arita (unpublished).

Arima (1975) at atmospheric pressure with special reference to the solubility of Al_2O_3 in protoenstatite above 1300°C. The phase equilibrium diagram is given in Fig. 2. MgATs is incorporated in protoenstatite as much as 3.5 wt.% (1.75 wt.% Al_2O_3), in an agreement with the observation of Bigger and Clark (1973). At subsolidus temperature the phase assemblage protoenstatite+forsterite was confirmed in the compositional range from En(96.5)MgATs(3.5) to En(94.5)MgATs(5.5). The presence of this field indicates that the composition of protoenstatite$_{ss}$ extends over an area on both sides of the join En-MgATs on the ternary plane of MgO-Al_2O_3-SiO_2 as shown in Fig. 3 (probably protoenstatite$_{ss}$ is nonstoichiometric). In the more aluminous region the subsolidus phase assemblages are protoenstatite$_{ss}$+forsterite+cordierite$_{ss}$ and forsterite$_{ss}$+cordierite$_{ss}$+spinel. The unit cell parameters *a*, *b* and *V* of protoenstatite$_{ss}$ decrease with increasing Al_2O_3 content in it. In their discussion Onuma and Arima (1975) showed that the Al_2O_3 content of protoenstatite can be used as an indicator of temperature only above 1400°C, and that when the Al_2O_3 content is less than 2 wt.% it can not be used either as a pressure or temperature indicator.

The join $MgSiO_3$-$MgAl_2SiO_6$ at high pressures.

The join $MgSiO_3$-$MgAl_2SiO_6$ was studied by Arima and Onuma (1977) in the pressure and temperature range 10 – 25 Kb and 1100 – 1500°C, with special reference to the solubility of Al_2O_3 in enstatite. The T-X sections at 10, 15, 20, and 25 Kb are shown in Fig. 4. At subsolidus temperatures, the solubility of Al_2O_3 increases with increasing temperature. At 1450°C and 15 Kb MgATs is incorporated in enstatite as much as 33 wt.% (16.5 wt.% Al_2O_3). The P-T diagrams of the both compositions En(80)MgATs(20) and En(70)MgATs(30) are given in Fig. 5. The two univariant reactions, enstatite(En)+sillimanite(Sill) = sapphirine(Sa)+quartz(Qtz) and pyrope(Py) = En+Sill+Sa were determined experimentally. The temperature and pressure values of these univariant lines are in a good agreement with those determined by previous workers (Boyd 1959, Chatterjee and Schreyer 1972, Newton 1972). As shown in Fig. 6, these univariant lines do not intersect each other, indicating the metastable invariant point where En, Sa, Sill, Py, and Qtz coexist. The P-X sections of the join En-MgATs at various temperatures are given in Fig. 7. The pressure dependence of the solubility of Al_2O_3 is variable with respect to the coexisting minerals. The solubility decreases with increasing pressure when enstatite coexists with pyrope or with sillimanite+sapphirine, but increases with increasing pressure when enstatite coexists with sapphirine+quartz. From these experimental results, the Al_2O_3 content of orthopyroxene

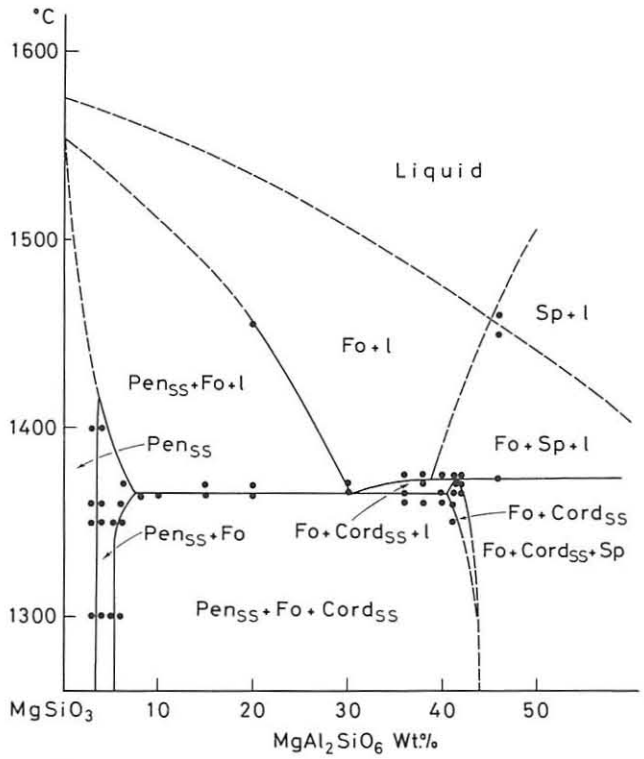

Fig. 2 Phase equilibrium diagram of the join $MgSiO_3$-$MgAl_2SiO_6$ at 1 atm. Pen, protoenstatite; forsterite; Cord, cordierite; Sp, spinel; l, liquid. (after Onuma and Arima, 1975).

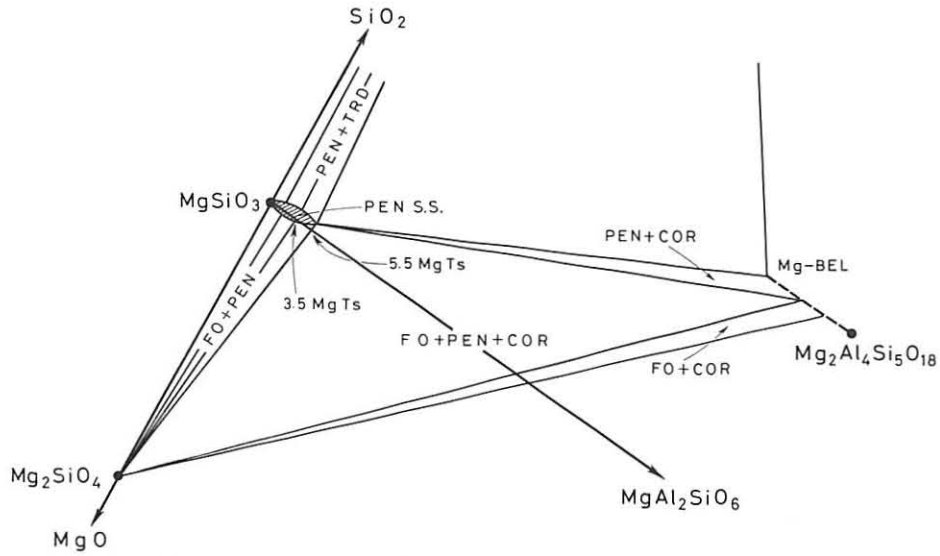

Fig. 3 A part of subsolidus diagram of the system MgO-Al_2O_3-SiO_2. PEN, protoenstatite; FO, forsterite; TRD, tridymite; COR, cordierite. (after Onuma and Arima, 1975).

can not be used as a pressure indicator without taking the mineral assemblage into account. The unit cell parameters of the synthetic enstatites were determined as shown in Figs. 17, 18, and 19. The unit cell edges *a*, *b* and the cell volume *V* decrease with increasing Al_2O_3 content in it, while no significant change was observed on the cell edge *c*.

Experimental methods

High pressure experiments were carried out with the piston cylinder apparatus with working volume of 1.25 cm in diameter and 5.00 cm in length. The pressure transmitting mediums were molten pyrex glass and sodium chloride as shown in Fig. 8. Pt-Pt87Rh13 thermocouples were used for

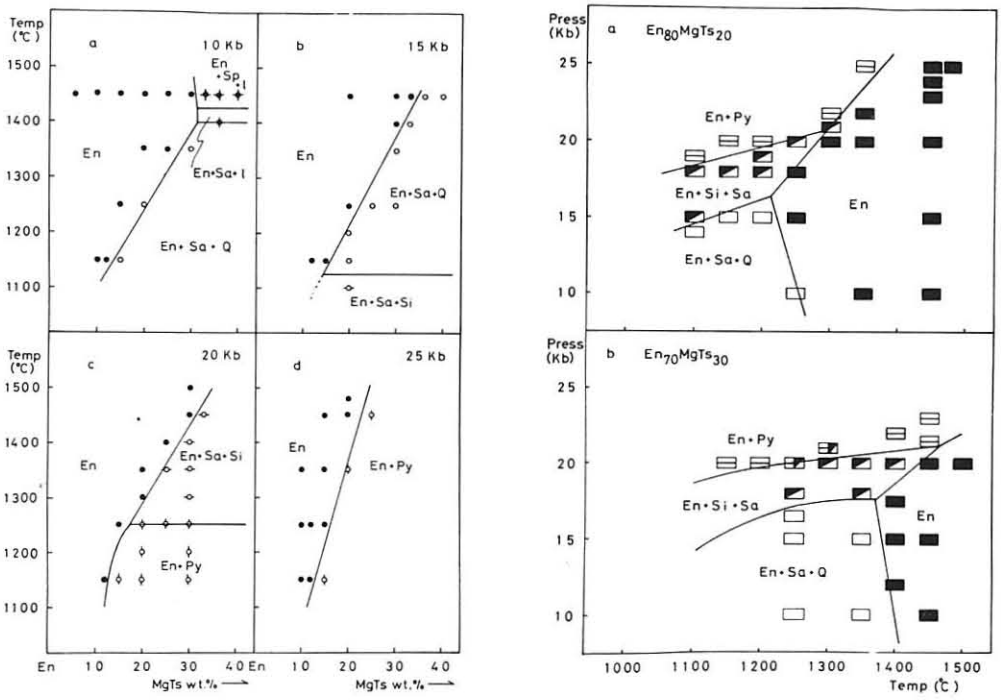

Fig. 4 (left) T-X sections in the join $MgSiO_3$-$MgAl_2SiO_6$ at 10, 15, 20, and 25 Kb. En, enstatite$_{ss}$; Sa, sapphirine$_{ss}$, Si, sillimanite; Q, quartz; sp, spinel; Py, pyrope; 1, liquid. (after Arima and Onuma 1977).

Fig. 5 (right) P-T diagrams at the isocompositional planes in En(80)MgATs(20)(top) and En(70)MgAts(30)(bottom). Abbreviations are given in Fig. 4. (after Arima and Onuma 1977).

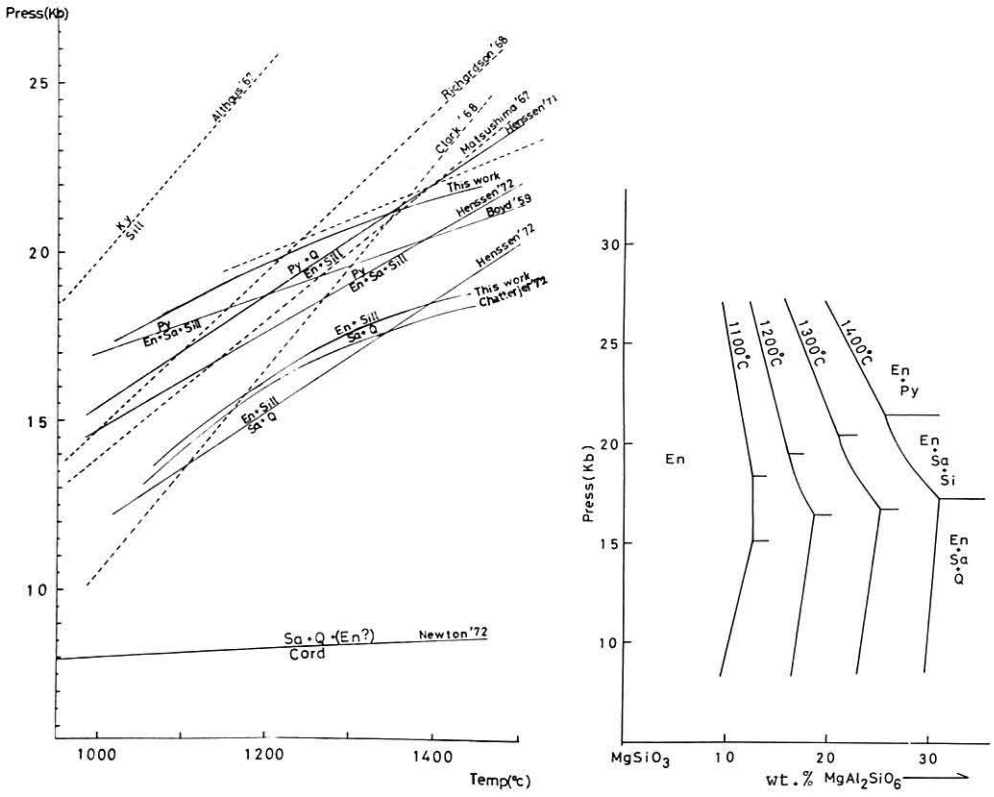

Fig. 6 (left) Comparison of the determinations of the univariant lines. (after Arima and Onuma 1977).

Fig. 7 (right) P-X sections in the join $MgSiO_3$-$MgAl_2SiO_6$. Abbreviations are given in Fig. 4. (after Arima and Onuma 1977).

temperature measurement. Temperature accuracy was estimated as ±10°C. The correction for pressure dependence of e.m.f. of the thermocouples was ignored. The pressure calibration was made by the same method as that described by Hariya et al. (1969). To keep oxidate state of iron as trivalent, oxide starting materials were prepared from reagents of Fe_2O_3, Al_2O_3, MgO, and SiO_2, grounded in an agate mortar with ethylalcohole for 4 hours. In the pressure cell, graphite reacts with water from pressure transmitting talc by the following equations.

$$C+O_2 = CO_2$$
$$H_2O = H_2 + \frac{1}{2} O_2$$

H_2 is permiable through the Pt wall of the sample capsule and makes the low oxygen partial pressure in the sample capsule. Under such low oxygen pressure buffered by these reactions, the experimental products at 1000°C and 10 Kb in

the join En-$MgFe^{3+}AlSiO_6$ (MgFATs) were the assemblage of orthopyroxene+olivine+magnetite and the one phase field of orthopyroxene was not encountered. These results indicate the presence of Fe^{2+} in the run products and the composition of the run products containning olivine and magnetite are no longer on the join En-MgFATs. To keep high oxygen pressure in the sample capsule, the double capsules buffering method proposed by Ohashi and Hariya (1973) was employed. As shown in Fig. 8, starting material was containned in the sealed Pt inner capsule with 20 wt.% water, and PtO_2 buffer material was put into the sealed Pt outer capsule with 10 wt.% water. The length and diameter of the inner and outer capsules were 5.00 mm and 2.30 mm, and 10.0 mm and 3.5 mm respectively. After the run PtO_2 and Pt_3O_4 were identified in the outer capsule by using a X-ray diffractometer. According to the experimental study by White (1971), the reaction $3PtO_2 = Pt_3O_4 + O_2$ make the very high oxygen pressure at high temperatures. In the temperature and pressure range of the present experiment, hematite(Hem) was encountered in the run product when PtO_2 and Pt_3O_4 were identified after the run. When neither PtO_2 nor Pt_3O_4 was confirmed, magnetite appeared in the run product. The experimental products containning magnetite were excluded out from the present discussion.

The experimental products were examined by the aid of an optical microscope and a X-ray diffractometer.

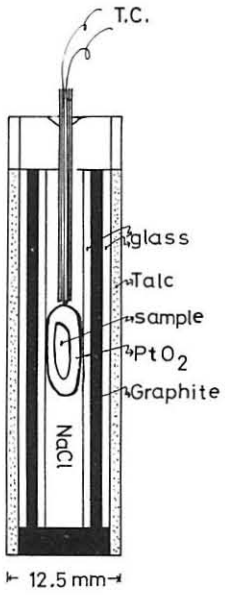

Fig. 8 Schematic diagram of high pressure cell.

Table 1. Experimental results

Composition (wt.%)		Temp. (°C)	Press. (Kb)	Time (hr)	Results
$MgSiO_3$	$MgFe^{3+}AlSiO_6$				
97.5	2.5	1100	16	49	En and rare Hem
97.5	2.5	1150	16	42	En only
97.5	2.5	970	12	45.5	En and rare Hem
97.5	2.5	1020	12	48.5	En only
97.5	2.5	920	8	48	En only
97.5	2.5	880	8	47	En only
97.5	2.5	800	8	69	En and rare Hem
95.0	5.0	1200	8	22.4	En only
95.0	5.0	950	8	46	En and rare Hem
95.0	5.0	1000	8	41	En and rare Hem
95.0	5.0	1050	8	46	En only
95.0	5.0	1100	12	29	En only
95.0	5.0	1000	12	44	En and rare Hem
95.0	5.0	1050	12	27.7	En and rare Hem
95.0	5.0	1200	16	21.4	En only
95.0	5.0	1250	16	19.8	En only
95.0	5.0	1100	16	22	En and Hem
95.0	5.0	1150	16	22.2	En only
92.5	7.5	1150	8	4.6	En only
92.5	7.5	1100	12	20	En and Hem
92.5	7.5	1200	12	26	En only
92.5	7.5	1250	8	22.5	En only
92.5	7.5	1000	5	46.5	En and rare Hem
92.5	7.5	1250	16	19.5	En and small amount Hem
92.5	7.5	1220	16	22	En only
92.5	7.5	1175	16	22.4	En, rare Hem and trace 01
92.5	7.5	1150	8	20	En only
90.0	10.0	1100	8	22	En and rare Hem
90.0	10.0	1200	8	21.5	En only
90.0	10.0	950	8	24	En and Hem
90.0	10.0	1150	8	21.4	En and Hem
90.0	10.0	1100	12	22	En and rare Hem
90.0	10.0	1200	12	19	En and rere Hem
90.0	10.0	1250	12	10.4	En and trace 01
90.0	10.0	1000	10	74	En and Hem
90.0	10.0	1200	16	22.8	En and Hem
90.0	10.0	1250	16	4	En and rare Hem
90.0	10.0	1400	12	6	En and X phase (inclusion)
85.0	15.0	1100	8	22	En and Hem
85.0	15.0	1000	8	47	En and Hem
85.0	15.0	1300	8	8	En and rare Hem
70.0	30.0	1050	8	69	En and Hem
70.0	30.0	950	8	95.	En, Hem and trace Sp
70.0	30.0	850	8	69	En, Hem and trace Sp
70.0	30.0	1000	12	29.5	En, Hem and trace Sp
70.0	30.0	1050	12	22	En and Hem
65.0	35.0	1000	8	42	En, Hem rare Sp
65.0	35.0	1100	8	26	En, Hem and rare Sp
65.0	35.0	1150	8	21.3	En, Hem and rare Sp
65.0	35.0	1200	8	21	En and Hem

Table 1. (continued)

Composition			Temp.	Press.	Time	Results
(wt.%)			(°C)	(Kb)	(hr)	
$MgSiO_3$	$MgFeAlSiO_6$					
60.0	40.0		1000	8	47	En, Hem and small amount Sp
$MgSiO_3$	$MgFe^{3+}_{2/3}Al_{4/3}SiO_6$					
80.0	20.0		1150	12	18	En, Hem and trace 01
80.0	20.0		1100	12	24.4	En and rare Hem
80.0	20.0		1150	12	22	En rare Hem and trace Sp
85.0	15.0		1050	12	24.5	En rare Hem
85.0	15.0		1100	12	20.4	En only
85.0	15.0		1100	16	21	En and rare Hem
85.0	15.0		1150	16	21.5	En only
90.0	10.0		1000	12	33.5	En only
90.0	10.0		950	12	42.5	En and rare Hem
$MgSiO_3$	Al_2O_3	Fe_2O_3				
90.0	7.5	2.5	1100	8	20.5	En rare Sa and trace Qtz
92.0	6.0	2.0	1100	8	21.4	En only
Reversal run						
$MgSiO_3$	$MgFe^{3+}AlSiO_6$					
95.5	5.0		1000	8	25.5	En → En and rare Hem
92.5	7.5		1050	8	21.4	En → En and rare Hem

Abbreviations, En, enstatite$_{ss}$; Hem, hematite; Sp, spinel$_{ss}$; Qtz, quartz; Sa, sapphirine$_{ss}$; Ol, olivine.

Some selected reversal run were carried out. The experimental results are given in Table 1. The crystalline mixture of enstatite single phase synthesized from oxide starting material was heated again at the temperature and pressure condition where enstatite$_{ss}$ and hematite were synthesized from the oxide starting materials. After the reversal run, small amount of hematite appeared. These reasults indicate that the concentration of Al_2O_3 and Fe_2O_3 in enstatite determined in the present experiments was in equilibrium.

Experimental results

High pressure experiments

High pressure experiments were carried out in the pressure and temperature range 8 – 16 Kb and 800 – 1300°C. The experimental results are listed in Table 1.

The T-X sections in the join En-MaFATs at 8, 12, and 16 Kb are given in Figs. 9, 10, and 11. At 8 Kb enstatite$_{ss}$, spinel(Sp)$_{ss}$, and Hematite were encountered (Fig. 9). The solubility of MgFATs in enstatite increases with increasing temperature. The maximum solubility of MgFATs confirmed in this experiment was 10 wt.% at 1200°C. The solvus is presented as a straight line at higher temperature region above 1000°C and as a curved line at lower temperature below 1000°C. Only 1 wt.% MgFATs is incorporated in enstatite below 800°C. In the more MgFATs compositional region, the assemblage En_{ss}+Hem was encountered. This results indicates the following reaction.

$$\underset{En_{ss}}{2MgFe^{3+}AlSiO_6} = \underbrace{\underset{En_{ss}}{MgAl_2SiO_6} + MgSiO_3}_{} + \underset{Hem}{Fe_2O_3} \qquad \text{Eq. 1}$$

The assemblage En_{ss}+Sp_{ss}+Hem was confirmed in the experimental products in the more MgFATs compositional part. These results indicate the limit of the solubility of Al_2O_3 in enstatite and the following reaction.

$$\underset{En_{ss}}{MgAl_2SiO_6} = \underset{Sp_{ss}}{MgAl_2O_4} + \underset{Qtz}{SiO_2} \qquad \text{Eq. 2}$$

The boundary curve between the field of En_{ss}+Hem and that of En_{ss}+Sp_{ss}+Hem was determined as shown in Fig. 9. Pale green color of this spinel phase indicates the presence of iron in it. The coexistence of hematite with spinel phase indicates the presence of magnesioferrite ($MgFe_2^{3+}O_4$) rather than that of

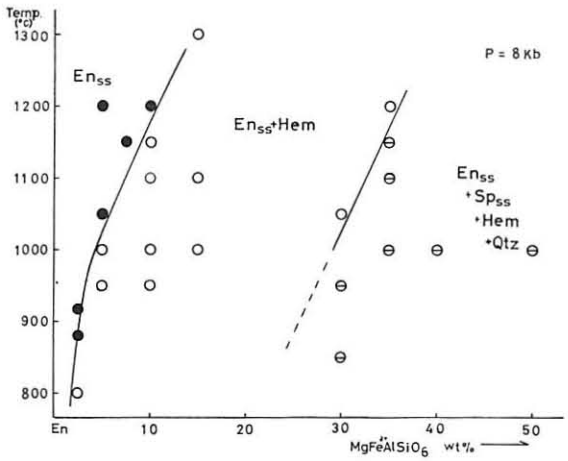

Fig. 9 T-X section at 8 Kb in the join $MgSiO_3$-$MgFe^{3+}AlSiO_6$. En_{ss}, enstatite$_{ss}$; Hem, hematite; Sp_{ss}, spinel$_{ss}$; Qtz, quartz.

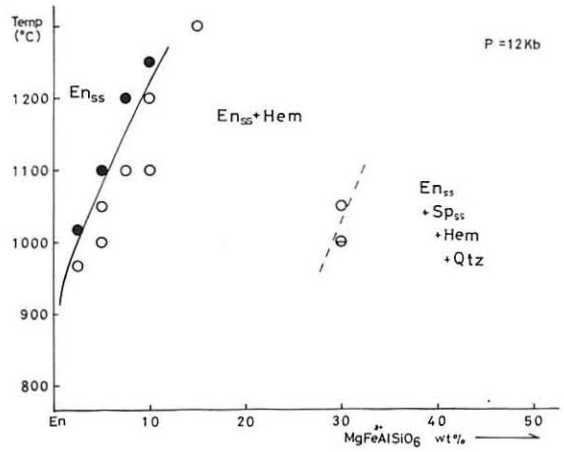

Fig. 10 T-X section at 12 Kb in the join $MgSiO_3$-$MgFe^{3+}AlSiO_6$. Abbreviations are given in Fig. 9.

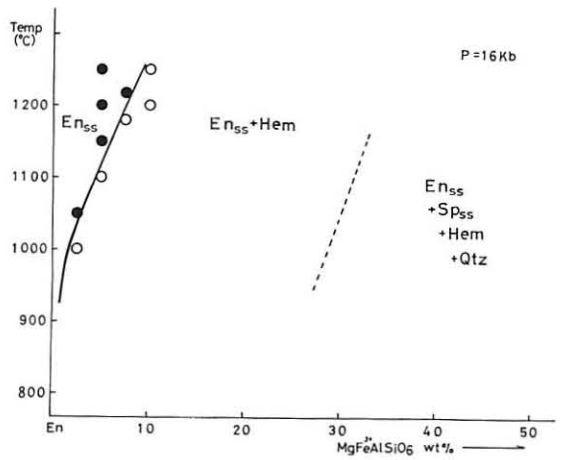

Fig. 11 T-X section at 16 Kb in the join $MgSiO_3$-$MgFe^{3+}AlSiO_6$. Abbreviations are given in Fig. 9.

magnetite ($Fe^{2+}Fe^{3+}_2O_4$) or hercynite ($Fe^{2+}Al_2O_4$) in it structure. $Spinel_{SS}$ coexisting with hematite and $enstatite_{SS}$ is attributed by the following reaction.

$$MgFe^{3+}_2O_4 + SiO_2 = MgSiO_3 + Fe_2O_3 \qquad \text{Eq. 3}$$
$$Sp_{SS} \quad Qtz \quad En_{SS} \quad Hem$$

The change of $\Delta 2\theta$ of $enstatite_{SS}$ in the variable compositions of the run materials at 1000°C were determined as shown in Fig. 13. In the single phase field of En_{SS} and the two phase field of En_{SS}+Hem, the $\Delta 2\theta$ increases with increasing MgFATs in the run materials indicating that Al_2O_3 and Fe_2O_3

contents of enstatite$_{ss}$ increase. In four phase field of En_{ss}+Sp_{ss}+Hem+Qtz, however, it is a constant value indicating the fixed composition of enstatite$_{ss}$, which is determined by the invariant reactions of Eqs. 2 and 3. Though quartz was not confirmed in the run materials, its presence was theoretically assumed. Rare amount of spinel in these run products implied that quartz is probably present in trace amount and it is difficult to identify the presence of quartz.

At 12 Kb (Fig. 10), the single phase field of En_{ss}, the two phase field of En_{ss}+Hem, and the assemblage of En_{ss}+Sp_{ss}+Hem(+Qtz) were encountered. The solvus was determined as a straight line in the temperature range 1000 – 1250°C. The boundary curve between the field of En_{ss}+Hem and that of En_{ss}+Sp_{ss}+Hem+Qtz was determined in the composition of En(70)-MgFATs(30) at 1025°C, and its slope was presented on the analogy of that determined at 8 Kb.

At 16 Kb (Fig. 11), the single phase field of En_{ss} and the two phase field of En_{ss}+Hem were encountered. Though no experiment was made in the part with high MgFATs content of this join, the boundary between the field of En_{ss}+Hem and that of En_{ss}+Sp_{ss}+Hem+Qtz is provisionally given by the

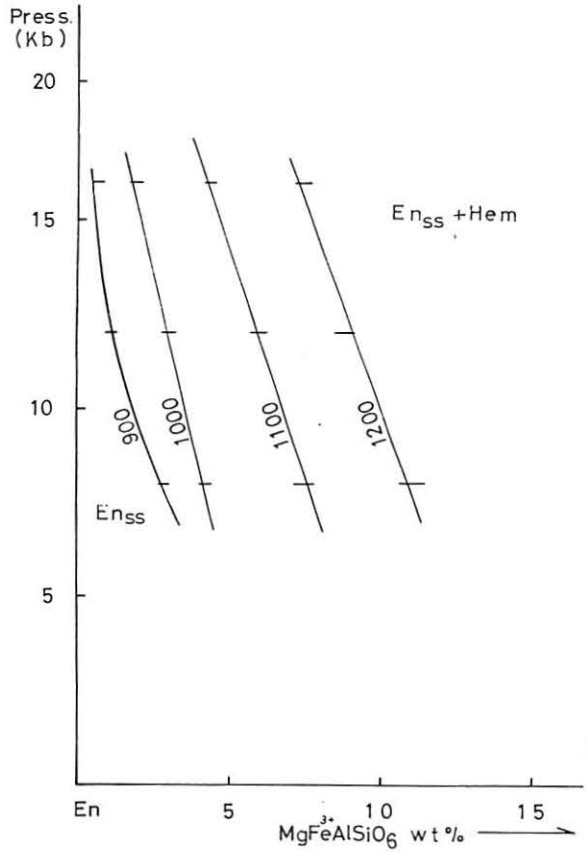

Fig. 12 P-X sections in the join $MgSiO_3$-$MgFe^{3+}AlSiO_6$. Abbreviations are given in Fig. 9.

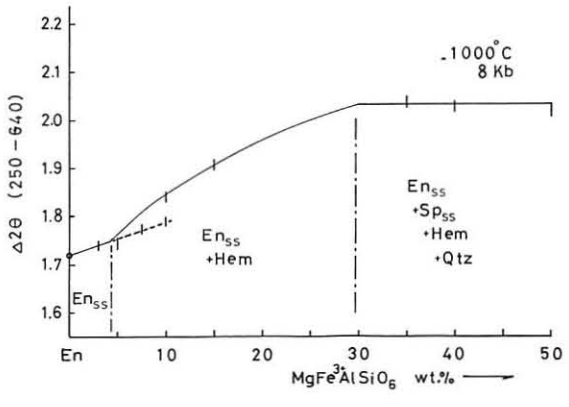

Fig. 13 The relationship between $\Delta 2\theta$ of the enstatite$_{ss}$ and bulk composition at 1000°C and 8 Kb. Broken line indicates $\Delta 2\theta$ of enstatite$_{ss}$ in the enstatite single phase field at higher temperature than 1000°C.

consideration of the pressure and temperature dependence of this curve determined at 8 and 12 Kb.

The phase equilibria in the more aluminous join $MgSiO_3$-$MgFe^{3+}_{2/3}Al_{4/3}SiO_6$ ($MgFA_2Ts$) were studied experimentally in the pressure and temperature range 12 – 16 Kb and 950 – 1150°C, for the purpose to determine the single phase field of enstatite$_{ss}$. The T-X section in the part with lower $MgFA_2Ts$ content of this join at 12 Kb is given in Fig. 14. The single phase field of En_{ss} and the two phase field of En_{ss}+Hem were encountered. The boundary curve between these field was determined as a straight line between 950 – 1150°C. The single phase field of En_{ss} expands with increasing temperature. The solvus at 16 Kb was determined experimentally to pass through a poin of En(85)$MgFA_2Ts$(15) at 1125°C as shown in Fig. 15. In this join a reaction of Eq. 1 also takes place and the temperature and pressure dependences of Eq. 1 determined in this join are in a good agreement with that determined in the join En-MgFATs. In Fig. 15 the boundary between the field of En_{ss} and that of En_{ss}+Hem at 8, 12, and 16 Kb are given. Ths single phase field of En_{ss} decreases with increasing pressure and decreasing temperature.

Some high pressure experiments were carried out at 1100°C and 8 Kb in the two compositions of En(90)Al_2O_3(7.5)Fe_2O_3(2.5) and En(92)Al_2O_3-(6.0)Fe_2O_3(2.0). The experimental results are given in Table 1. In the later composition only enstatite$_{ss}$ was encountered and in the former the assemblage of En_{ss}+Sa_{ss}+Qtz was encountered. These results indicate that the following reactions are present between these two compositions at 1100°C and 8 Kb.

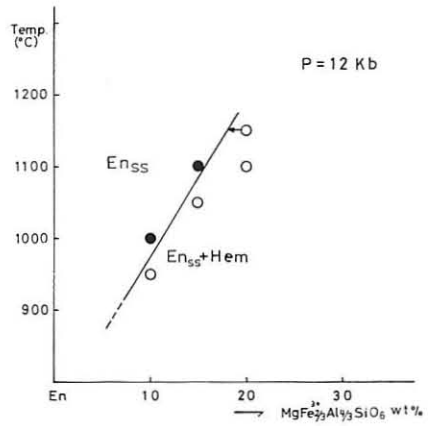

Fig. 14 T-X section at 12 Kb in the join En-$MgFA_2Ts$.

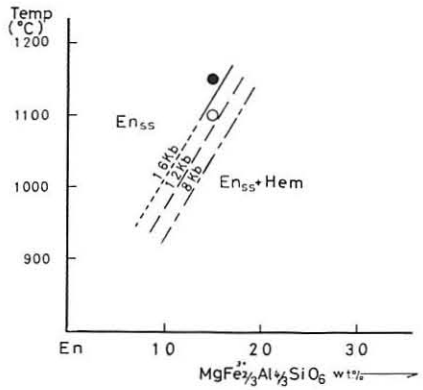

Fig. 15 T-X sections at 8, 12, and 16 Kb in the join En-$MgFA_2Ts$.

$$\underset{En_{SS}}{MgFe^{3+}AlSiO_6} = \frac{1}{4}\underbrace{Mg_2Al_4SiO_{10} + \frac{1}{4}Mg_2Fe^{3+}_4SiO_{10}}_{Sa_{SS}} + \underset{Qtz}{\frac{1}{2}SiO_2} \qquad \text{Eq. 5a}$$

$$\underset{En_{SS}}{MgAl_2SiO_6} = \frac{1}{2}\underset{Sa_{SS}}{Mg_2Al_4SiO_{10}} + \underset{Qtz}{\frac{1}{2}SiO_2} \qquad \text{Eq. 5b}$$

The solubility of Al_2O_3 in enstatite determined by Eq. 5b in the ternary system MgO-Al_2O_3-SiO_2 has been determined by Arima and Onuma (1977). The subsolidus phase equilibria diagram in the MgO-Al_2O_3-Fe_2O_3-SiO_2 at 1100°C and 8 Kb is given in Fig. 16. The solubility of Al_2O_3 in enstatite coexists with sapphirine and quartz in the Fe^{3+} bearing system is much more than that of enstatite in the ternary system MgO-Al_2O_3-SiO_2. This result indicates that Al_2O_3 is incorporated in enstatite by the substitution MgSi = AlAl as well as MgSi = Fe^{3+}Al in the Fe^{3+} bearing system. At 1100°C and 8 Kb, the solubility of Al_2O_3 is about 5 wt.% in the ternary system MgO-Al_2O_3-SiO_2 and maximum value is 6.5 wt.% in the quaternary system MgO-Al_2O_3-Fe_2O_3-SiO_2.

Crystalline phases

$Enstatite_{SS}$, $spinel_{SS}$, $sapphirine_{SS}$ hematite, and quartz were identified by the aid of a X-ray diffractometer and an optical microscope.

$Enstatite_{SS}$ forms euhedral crystal, up to 30μ in size, pale yellow in color, needle like shaped at lower temperature around 900°C and elongated recutangular or rounded shaped at higher temperature around 1100°C. The

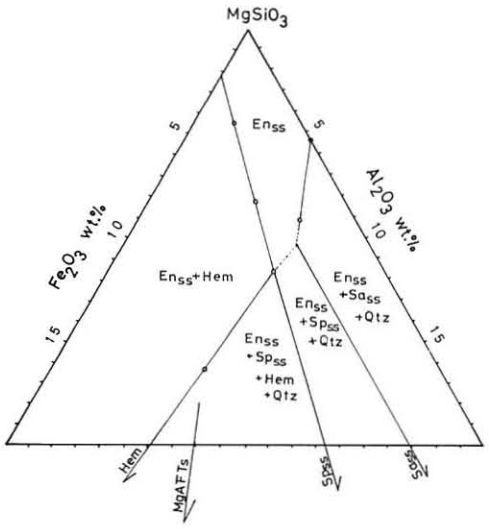

Fig. 16 The subsolidus phase diagram in the system $MgSiO_3$-Al_2O_3-Fe_2O_3 at 1100°C and 8 Kb. Abbreviations are given in Fig. 9.

unit cell parameters of enstatites were determined by using the following diffraction lines, (060), (10,31), (250), (541), (640), (621), (631), (241), (820), (721), (531), and (630). Silicon was used as an external standard. The cell parameters given in Table 2 were calculated by using the UNICS computer program by Sakurai (1968). In Figs. 17, 18, and 19 the cell edges *a*, *b*, and *c* and the cell volume *V* of enstatites synthesized in the system $MgSiO_3$-Al_2O_3-Fe_2O_3 are given with those of enstatites synthesized in the system $MgSiO_3$-Al_2O_3 by Skinner and Boyd (1964) and Arima and Onuma (1977). The cell edges *a* and *c* show no significant change in the narrow compositional range of the join En-MgFATs and En-$MgFA_2$Ts as shown in Fig. 18. The cell edge *b* and the cell volume *V* decrease with increasing MgFATs or $MgFA_2$Ts content of enstatite. Figs. 17, 18, and 19 show that Fe^{3+} bearing enstatite has the larger cell edges *b* and *a* and the larger cell volume *V* than those of Fe^{3+} free enstatite, as supported by the larger ionic radius of Fe^{3+} than that of Al. These results indicate that the subsitution MgSi = Fe^{3+}Al makes a weak decrease of cell volume compared with that made by the substitution MgSi = AlAl.

EPMA chemical analyses were carried out on some synthetic enstatites. The results are listed in Table 3. Enstatite crystals analyzed were present as a single phase in the run products except the run product of En(80)$MgFA_2$Ts(20) consisting of En_{SS}+Hem. Fine grain of enstatite crystals (up to 30μ, average 10μ) made it difficult to analyze by EPMA. The chemical compositions determined show a variation in the range of ±1.0 wt.%. These variations could

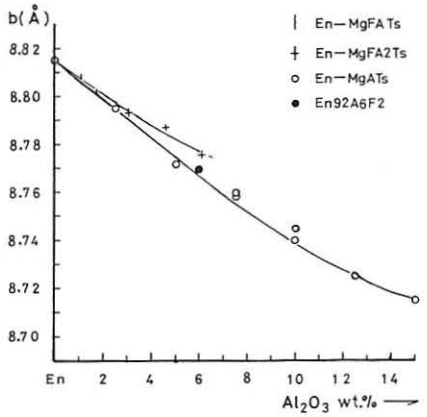

Fig. 17 The relationship between the unit cell edge b and the Al_2O_3 content of synthetic enstatite$_{ss}$.

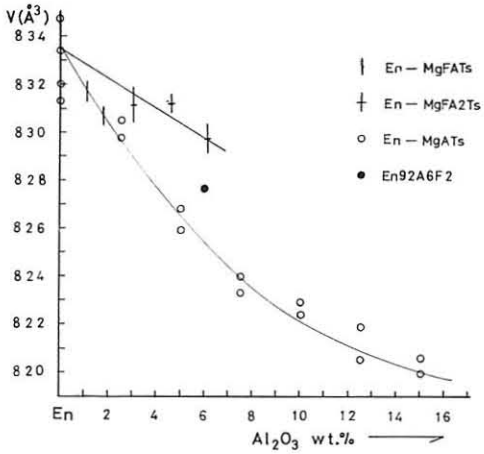

Fig. 19 The relationship between the unit cell volume V and the Al_2O_3 content of synthetic enstatite$_{ss}$.

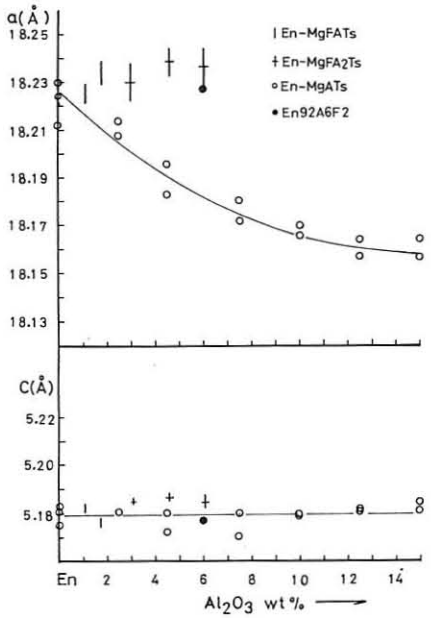

Fig. 18 The relationship between the unit cell edges a and c and the Al_2O_3 content of synthetic enstatite$_{ss}$.

be attributed to the analytical error caused by a fine grain of enstatite crystals. The composition of enstatite in the run product in En(92.5)MgFATs(7.5) at 1220°C and 16 Kb, and that at 1200°C and 12 Kb show more SiO_2 and less MgO than these of planned composition. The chemical formulas of these enstatites imply the presence of $Fe^{2+}SiO_3$ in them. On the other hand the chemical composition and the formula of the enstatite synthesized at 1150°C and 12 Kb show a good agreement with those of planned composition. This agreement was also confirmed in the analytical result in En(85)$MgFA_2$Ts(15) at 1100°C and 8 Kb. Mössbauer spectra on the enstatite synthesized at 1400°C and 12 Kb indicate that high temperature around 1400°C is not favourable to the presence of Fe^{3+} in enstatite. There is a probability of the presence of some amount of $Fe^{2+}SiO_3$ in enstatite synthesized above 1200°C. The composition of the enstatite coexisting with hematite in the run product of En(80)$MgFA_2$-Ts(20) was determined by EPMA. The composition of this enstatite is plotted in the more aluminous region than that of the starting material. This result is explained by the reaction of Eq. 1. The composition of enstatite coexisting with hematite is plotted on the tie line of hematite-starting material in the system $MgSiO_3$-Al_2O_3-Fe_2O_3. The single phase field of enstatite$_{ss}$ in the join En-$MgFA_2$Ts at 1150°C and 12 Kb was determined as shown in Fig. 14 by using this EPMA analytical result and the compositional relation among En_{ss}, Hem, and starting material.

Spinel$_{ss}$ forms octahedral crystal, 1μ in size. Pale green color indicates the presence of iron in it. It is easily distinguished from other phases by its high refractive index and isotropic property under the optical microscope. Because of the lower intensity of the diffraction lines and the presence of the other phases, it was impossible to determine the unit cell parameter hence its compositional change.

Hematite appeared as euhedral crystals. No shift of its X-ray diffraction line was observed suggesting the fixed composition close to Fe_2O_3.

Sapphirine$_{ss}$ was observed only optically in the run product of En(90)Al_2O_3(7.5)Fe_2O_3(2.5) at 1100° and 8 Kb. Fine grained euhedral crystals, brown in color were identified. Quartz was identified by the aid of a X-ray diffractometer in the same run product. In the assemblage of En_{ss}+Sp_{ss}+Hem, it was unsuccessful to find out the presence of quartz optically.

The Mössbauer spectra of the synthetic enstatites

The Mössbauer spectra measurements were made on the two synthetic enstatites containning 3.5 wt.% Fe_2O_3 synthesized at 1150°C 8 Kb, and

Table 2 Cell parameters of synthetic enstatites

Composition (wt.%)			a(Å)	b(Å)	c(Å)	V(Å^3)
En	MgFATs					
95.0	5.0		18.225±0.004	8.808±0.001	5.182±0.002	831.8±0.4
92.5	7.5		18.234±0.005	8.802±0.001	5.176±0.002	830.7±0.5
90.0	10.0		18.233±0.009	8.800±0.005	5.183±0.003	831.7±0.8
En	MgFA2Ts					
90.0	10.0		18.230±0.008	8.793±0.002	5.185±0.005[a]	831.3±0.9
85.0	15.0		18.238±0.006	8.787±0.001	5.186±0.002	831.2±0.3
80.0	20.0		18.236±0.007	8.776±0.002	5.185±0.003	829.81±0.7
En	Al_2O_3	Fe_2O_3				
92.0	6.0	2.0	18.229±0.008	8.769±0.002	5.177±0.004	827.6±0.8

1400°C 12 Kb.

In Fig. 20, the computer plot of the Mössbauer spectra of the enstatite synthesized at 1150°C and 8 Kb is given. The spectra consist of two doublets which have chemical shift(Cs) 0.17 mm/sec and 0.36 mm/sec, quadropole splitting(QS) 1.42 mm/sec and 0.94 mm/sec, respectively. According to the crystallographic study by Takeda (1972) on the Takashima bronzite (2.67 wt.% Fe_2O_3 and 4.35 wt.% Al_2O_3), Fe^{3+} and Al are present in smaller octahedral site(M1) rather than larger octahedral site(M2) in orthopyroxene structure, and Al is also present in tetrahedral site(T). From this crystallographical data, the inner doublet is assigned for Fe^{3+} in (M1) site. The QS and CS values of this doublet resemble to those of other silicate minerals such as clinopyroxene and sapphirine (Table 4).

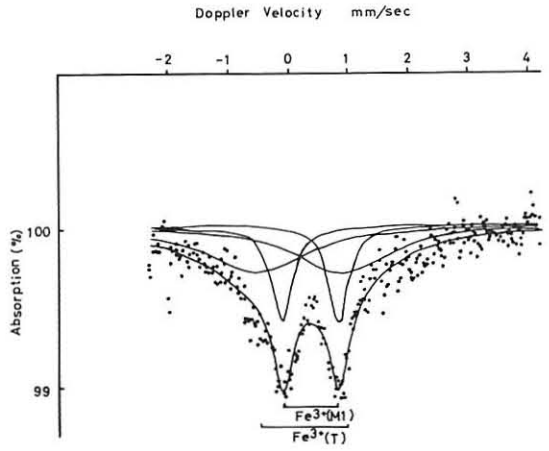

Fig. 20 The Mössbauer spectra of enstatite synthesized at 1150°C and 8 Kb.

Table 3 Chemical compositions of synthetic enstatites

Starting Material	En (85) $MgFA_2Ts$ (15)				
Temp. Press.	1150°C, 16 Kb				
Analytical No.	1	2	3	4	5
SiO_2	53.66	55.59	54.63	55.37	54.88
Al_2O_3	5.20	3.75	5.03	3.83	4.60
Fe_2O_3*	3.77	2.53	3.72	2.53	3.77
MgO	35.51	37.06	36.06	36.64	36.48
Total	98.14	98.93	99.44	98.37	99.73
Si	1.853	1.895	1.861	1.899	1.865
Al	0.212	0.152	0.203	0.154	0.184
Fe^{3+}	0.098	0.066	0.096	0.066	0.096
Mg	1.828	1.885	1.832	1.872	1.848

Starting Material	En (85) $MgFA_2Ts$ (15)		En (80) $MgFA_2Ts$ (20)		
Temp. Press.	1100°C, 12 Kb		1150°C, 12 Kb		
Analytical No.	1	2	1	2	3
SiO_2	54.51	54.30	53.91	53.39	54.66
Al_2O_3	5.44	4.55	5.17	5.61	5.71
Fe_2O_3*	3.90	3.53	3.97	4.02	3.53
MgO	35.99	35.73	35.52	34.27	35.72
Total	99.74	98.11	98.57	97.29	99.62
Si	1.853	1.870	1.855	1.860	1.857
Al	0.219	0.184	0.209	0.230	0.229
Fe^{3+}	0.100	0.101	0.103	0.105	0.090
Mg	1.826	1.832	1.822	1.778	1.808

Starting Material	En (92.5) MgFATs (7.5)				
Temp. Press.	1220°C, 16 Kb				
Analytical No.	1	2	3	4	5
SiO_2	58.21	58.59	57.53	59.01	57.60
Al_2O_3	1.21	1.56	1.60	1.20	1.58
Fe_2O_3*	1.79	1.97	2.19	1.54	2.38
MgO	37.94	37.90	37.11	37.61	37.34
Total	99.15	99.99	98.43	99.36	98.90
Si	1.972	1.969	1.967	1.990	1.961
Al	0.048	0.061	0.064	0.048	0.061
Fe^{3+}	0.045	0.049	0.055	0.039	0.061
Mg	1.916	1.898	1.891	1.890	1.894

Starting Material	En (92.5) MgFATs (7.5)		
Temp. Press.	1200°C, 12 Kb		
Analytical No.	1	2	3
SiO_2	60.25	58.15	58.61
Al_2O_3	1.17	2.24	2.11
Fe_2O_3*	2.20	2.34	2.97
MgO	37.19	36.45	36.83
	100.81	99.18	100.52
Si	2.002	1.970	1.974
Al	0.045	0.088	0.083
Fe^{3+}	0.055	0.060	0.074
Mg	1.845	1.827	1.817

* Total iron as Fe_2O_3

In some synthetic Fe^{3+}-bearing clinopyroxenes, the presence of Fe^{3+} in tetrahedral site has been reported (Shinno 1972, Ohashi and Hariya 1973). The Qs and Cs values of the outer doublet of synthetic enstatite resemble to those assigned for Fe^{3+} in (T) site of clinopyroxene as shown in Table 4. In Fig. 22, the single phase field of enstatite$_{ss}$ in the system $MgSiO_3$-Fe_2O_3 could be assumed as a narrow area at 1150°C (2 wt.% Fe_2O_3 could be incorporated in enstatite). This single phase field decreases with decreasing temperature. These experimental results indicate that $MgFe^{3+}_2SiO_6$ (Fe^{3+} in M1 and T sites) could be present at higher temperature. From these reasons the outer doublet may be assigned for Fe^{3+} in tetrahedral site of orthopyroxene structure. The lower absorption of the outer doublet than that of inner doublet indicates that Fe^{3+} strongly prefers (M1) site than (T) site. This assumption is supported by the unit cell parameters of this enstatite. The cell edge *c* does not show significant change expected by the replacement of smaller Si by larger Fe^{3+}. From the spectra of this enstatite, the presence of Fe^{2+} could not be confirmed.

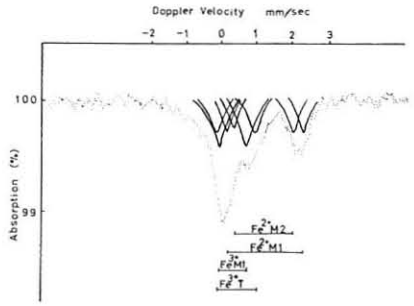

Fig. 21 The Mössbauer spectra of enstatite synthesized at 1400°C and 12 Kb.

The Mössbauer spectra of the enstatite synthesized at 1400°C and 12 Kb is shown in Fig. 21. On the basis of the data of Fe^{2+}bearing orthopyroxenes by Bancroft and Maddock (1967), Virgo and Hafner (1969) and those of the Fe^{3+} bearing enstatite mentioned above, it is estimated that there are four doublets assigned for Fe^{3+}(M1), Fe^{3+}(T), Fe^{2+}(M1), and Fe^{2+}(M2) in these spectra. The computed QS and CS values are listed in Table 4. The presence of Fe^{2+} in this enstatite makes it difficult to study the phase equilibria in the system $MgSiO_3$-Al_2O_3-Fe_2O_3 around 1400°C. From this result, the present experimental study was carried out only below 1300°C.

Table 4 Mössbauer spectra parameters of iron silicates

Mineral	Type of iron	Position in crystal structure	Apporoximate configuration of co-ordination site	Chemical shift (mm/sec.)	Quadrupole splitting (mm/sec.)
Fe-Mg olivine*	Fe^{2+}	M1, M2	Octa	1.25–1.27	2.89–3.02
Opx*	Fe^{2+}	M1	Octa	1.24–1.27	2.35–2.65
	Fe^{2+}	M2	Distorded Octa	1.22–1.27	1.91–2.13
Andradite*	Fe^{3+}		Octa	0.50	0.58
Epidote*	Fe^{3+}		Irregular Octa	0.43	2.01
Sapphirine*					
yellow	Fe^{3+}		Tetra	0.04	0.78
	Fe^{3+}		Tetra	0.37	1.37
blue	Fe^{3+}		Tetra	0.40	0.87
	Fe^{2+}		Octa	1.25	2.57
Cpx‡	Fe^{3+}	M1	Octa	0.63–0.74	1.12–0.91
	Fe^{3+}	T	Tetra	0.36–0.48	1.49–1.74
Opx	Fe^{3+}	M1	Octa	0.36	0.94
1150°C 8 Kb	Fe^{3+}	T	Tetra	0.17	1.42
Opx	Fe^{3+}	M1	Octa	0.45	0.50
1400°C 12 Kb	Fe^{3+}	T	Tetra	0.43	1.26
	Fe^{2+}	M1	Octa	1.19	2.37
	Fe^{2+}	M2	Distorded Octa	1.17	1.98

* from Bancroft and Maddock (1967, 1968)
‡ from Shinno (1972)

Discussions

Phase relations in the system $MgSiO_3$-Al_2O_3-Fe_2O_3

From the experimental results mentioned above, the diagram showing the single phase field of enstatite$_{ss}$ in the system $MgSiO_3$-Al_2O_3-Fe_2O_3 at 8 Kb and various temperatures is given in Fig. 22. At lower temperature than 900°C, only less than 1 wt.% Fe_2O_3 is expected to be incorporated in enstatite by the substitution MgSi = $Fe^{3+}Fe^{3+}$. Mössbauer spectra of the synthetic enstatite indicate the strong preference of Fe^{3+} to octahedral site than tetrahedral site. In Fig. 16, the solubility of Fe_2O_3 in enstatite at constant pressure and temperature increases with increasing Al_2O_3 content in it, indicating that Fe_2O_3 is mainly incorporated in enstatite by the substitution MgSi = Fe^{3+}Al. In natural orthopyroxenes, moreover, the presence of Fe^{3+} in tetrahedral site has not been reported. Therefore, in the present discussion $MgFe^{3+}_2SiO_6$ is ignored and $MgFe^{3+}AlSiO_6$ is considered as a reliable orthopyroxene molecule.

The present system is actually a join in the expanded quaternary system

MgO-Al_2O_3-Fe_2O_3-SiO_2. The phase relations in the join $MgSiO_3$-Al_2O_3-Fe_2O_3 of the system MgO-Al_2O_3-Fe_2O_3-SiO_2 at 1100°C and 8 Kb are given schematically in Fig. 23. At 1100°C and 8 Kb, following reactions were confirmed.

$$MgFe^{3+}AlSiO_6 = \frac{1}{2}\underbrace{MgAl_2SiO_6}_{En_{ss}} + \frac{1}{2}MgSiO_3 + Fe_2O_3 \qquad \text{Eq. 1}$$
$$En_{ss} \qquad\qquad En_{ss} \qquad\qquad Hem$$

$$MgAl_2SiO_6 = MgAl_2O_4 + SiO_2 \qquad \text{Eq. 2}$$
$$En_{ss} \qquad Sp_{ss} \qquad Qtz$$

$$MgSiO_3 + Fe_2O_3 = MgFe_2^{3+}O_4 + SiO_2 \qquad \text{Eq. 3}$$
$$En_{ss} \qquad Hem \qquad Sp_{ss} \qquad Qtz$$

$$2MgFe^{3+}AlSiO_6 = \underbrace{MgAl_2O_4 + MgFe_2^{3+}O_4}_{Sp_{ss}} + 2SiO_2 \qquad \text{Eq. 4}$$
$$En_{ss} \qquad\qquad Qtz$$

$$4MgFe^{3+}AlSiO_6 = \underbrace{Mg_2Al_4SiO_{10} + Mg_2Fe_4^{3+}SiO_{10}}_{Sa_{ss}} + 2SiO_2 \qquad \text{Eq. 5a}$$
$$En_{ss} \qquad\qquad Qtz$$

$$2MgAl_2SiO_6 = Mg_2Al_4SiO_{10} + SiO_2 \qquad \text{Eq. 5b}$$
$$En_{ss} \qquad Sa_{ss} \qquad Qtz$$

$$2MgAl_2O_4 + SiO_2 = Mg_2Al_4SiO_{10} \qquad \text{Eq. 6a}$$
$$Sp_{ss} \qquad Qtz \qquad Sa_{ss}$$

$$2MgFe_2^{3+}O_4 + SiO_2 = Mg_2Fe_4^{3+}SiO_{10} \qquad \text{Eq. 6b}$$
$$Sp_{ss} \qquad Qtz \qquad Sa_{ss}$$

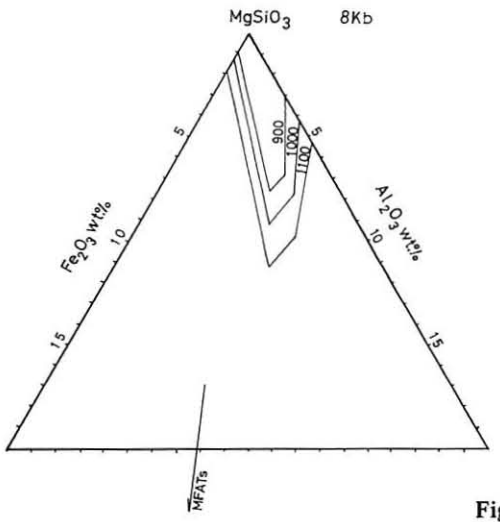

Fig. 22 The single phase field of enstatite$_{ss}$ at 8 Kb and various temperatures in the system $MgSiO_3$-Al_2O_3-Fe_2O_3.

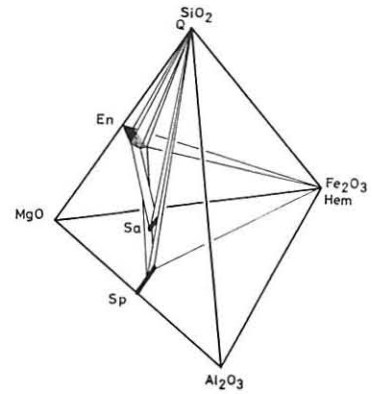

Fig. 23 The schematic diagram showing the phase relations in the system MgO-Al_2O_3-Fe_2O_3-SiO_2 at 1100°C and 8 Kb. Abbreviations are given in Fig. 9.

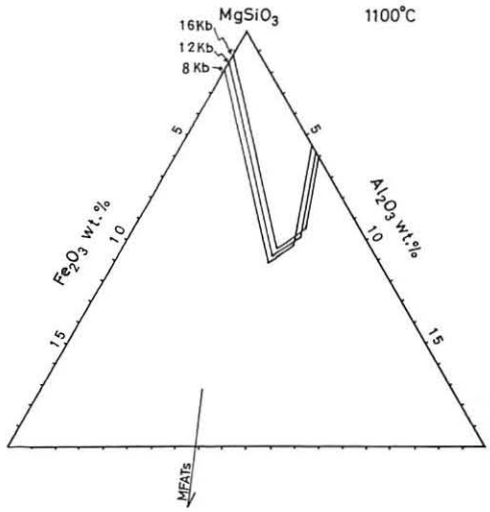

Fig. 24 The single phase field of enstatite$_{ss}$ at 1100°C and various pressures in the system $MgSiO_3$-Al_2O_3-Fe_2O_3.

Eq. 1 is an univariant reaction in the pseudoternary system $MgSiO_3$-Al_2O_3-Fe_2O_3 and the composition of enstatite$_{ss}$ coexisting with hematite is variable with respect to the bulk composition at constant temperature and pressure. The variable compositions of enstatites coexisting with hematite are indicated by the increase of $\Delta 2\theta$ of enstatite with increasing MgFATs and MgATs contents of run materials as shown in Fig. 13. The solubility of Fe_2O_3 in enstatite coexisting with hematite increases with increasing Al_2O_3 content in it, indicating that Fe_2O_3 is incorporated in enstatite by the substitution $MgSi = Fe^{3+}Al$. In four phase field of En_{ss}+Sp_{ss}+Hem+Qtz, there are two reactions of Eqs. 2 and 3. Eq. 2 is an invariant reaction in the ternary system MgO-Al_2O_3-SiO_2 and Eq. 3 is an invariant reaction in the quaternary system MgO-Al_2O_3-Fe_2O_3-SiO_2. By both reactions of Eqs. 2 and 3, the composition of enstatite$_{ss}$ and that of spinel$_{ss}$ are fixed. The $\Delta 2\theta$ of enstatite$_{ss}$ in the four phase field shows the constant value indicating its fixed composition as shown in Fig. 13.

Sharma et al. (1973) synthesized the spinel solid solution series between $MgAl_2O_4$ and $MgFe^{3+}_2O_4$ at 1300°C in air and stated the possibility of existence of solvus between them below 950°C at 7 Kb. However, since there is no experimental study on the relation between them at higher pressure than 7 Kb, the tie line between enstatite$_{ss}$ and spinel$_{ss}$ are presented provisionally as shown in Fig. 16.

Though no experiment was made in the compositional region where three phase field of En_{ss}+Sp_{ss}+Qtz is expected, this three phase field is presented as

shown in Fig. 16 on the basis of the experimental results in the other compositional region. In this field Eqs. 2 and 4 should be taking place.

In most aluminous region, the three phase field of En_{ss}+Sa_{ss}+Qtz is present as shown in Fig. 16. In this field there are two reaction of Eqs. 5a and 5b. Eq. 5b is an invariant reaction in the system MgO-Al_2O_3-SiO_2 and Eq. 5a is an univariant reaction in the system MgO-Al_2O_3-Fe_2O_3-SiO_2. The composition of enstatite$_{ss}$ is determined by these two reactions in this field. With increasing Fe_2O_3 content of enstatite$_{ss}$ coexisting with Sa_{ss}+Qtz, the solubility of Al_2O_3 in it strongly increases at constant pressure and temperature as shown in Fig. 16. This result indicates that the solubility of Al_2O_3 in enstatite depends on the Fe_2O_3 content of it as well as temperature and pressure variations. Therefore, the Al_2O_3 content of orthopyroxene can not be used as an indicator of temperature and/or pressure without taking the Fe_2O_3 content of it into account. On the other hand, the solubility of $MgAl_2SiO_6$ in enstatite is constant at constant temperature and pressure when it coexists with Sa_{ss}+Qtz as shown in Fig. 16. The increase of Al_2O_3 content of enstatite$_{ss}$ with increasing Fe_2O_3 content of it is attributed to the solubility of $MgFe^{3+}AlSiO_6$ in it. This results makes it possible to use the $MgAl_2SiO_6$ content as an indicator of temperature and/or pressure.

Present experimental results indicate that sapphirine breaks down to the assemblage of Sp_{ss}+Qtz in the part of high Fe_2O_3 content in the system

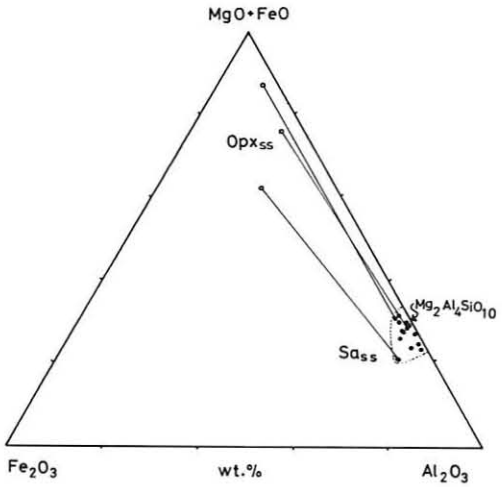

Fig. 25 The compositional relationships between natural orthopyroxenes and sapphirines in the system MgO-Al_2O_3-Fe_2O_3. A tie line indicates a coexisting relation. Sources of data, Segnit (1957), McKie (1963), Barker (1964), Lutts and Kopaneva (1967), Moore (1969), Haapala et al. (1971), Monchoux (1972), Merlino (1973), Woodford and Wilson (1976).

$MgO\text{-}Al_2O_3\text{-}Fe_2O_3\text{-}SiO_2$. This breaking down reaction is expressed by the Eqs. 6a and 6b. In fig. 25, Fe_2O_3/Al_2O_3 ratio of several natural sapphirines are plotted, implying the narrow field of sapphirine$_{SS}$ between $Mg_2Al_4SiO_{10}$ and $Mg_2Fe^{3+}_4SiO_{10}$. Though there is no experimental study on the relation between them, the presence of solvus is assumed and a tie line between Sa_{SS} and En_{SS} is presented as shown in Fig. 16.

The temperature and pressure dependence of the solubility of Al_2O_3 and Fe_2O_3 in enstatite

In Fig. 22, the single phase field of enstatite$_{SS}$ at various temperatures and 8 Kb are given. Independently of coexisting phases, the solubility of Al_2O_3 and Fe_2O_3 in enstatite increases with increasing temperature. Fig. 24 shows the single phase field of enstatite$_{SS}$ at 1100°C in the pressure range 8 – 16 Kb. The solubility of MgFATs slightly decreases with increasing pressure when enstatite coexists with hematite (Fig. 12). The pressure dependence of the solubility of MgATs in enstatite coexists with spinel$_{SS}$+quartz is estimated to be slight. From these data, the pressure dependence of the solubility of MgFATs in enstatite (maximum solubility) coexisting with sapphirine$_{SS}$+quartz is determined as shown in Fig. 24.

Geological applications

Al_2O_3 content of orthopyroxene has been given an attention by many investigators as a geobarometer and a geothermometer. The experimental studies have been made on the incorporation of Al_2O_3 in enstatite by the substitution MgSi = AlAl, and these experimental results have been used to estimate the pressure and/or temperature conditions of natural rocks (Boyd 1973, Hermans et al. 1976).

In general, natural orthopyroxenes show small amount of silica deficiency in these chemical formulas. These silica deficiencies are explained by the replacement of Si by Al in tetrahedral site and the corresponding replacement of Mg by Al in octahedral site(M1). This substitution of MgSi = AlAl leads to the hypothetical pyroxene molecule $MgAl_2SiO_6$ (MgATs). In chemical formulas of natural orthopyroxenes, Al in M1 site is generally less than Al in T site, and Cr, Ti, and Fe^{3+} are regarded to enter in M1 site, filling up the vacancy. These assumption lead to the hypothetical pyroxene molecules such as $MgCrAlSiO_6$, $MgTiAl_2O_6$. As shown in Fig. 1, some natural orthopyroxenes show both high contents of Al_2O_3 and Fe_2O_3 (exceed 2 – 3 wt.%), indicating the substitution MgSi = Fe^{3+}Al as well as MgSi = AlAl. While Cr_2O_3 and TiO_2 contents are

generally very low and scarcely exceed 1 wt.%. Therefore $MgCrAlSiO_6$ and $MgTiAl_2O_6$ molecules in natural orthopyroxenes are not so important with respect to the solubility of Al_2O_3 in orthopyroxenes.

Orthopyroxenes from volcanic rocks and plutonic differentiated rocks have both low Al_2O_3 and Fe_2O_3 contents as shown in Figs. 26 and 27, while from intrusive peridotites have high Al_2O_3 content. Figs. 26 and 27 show the low Fe_2O_3 and high Al_2O_3 contents of these orthopyroxenes. Fe_2O_3 content scarcely exceed 2 wt.% and amount of Fe^{3+} in M1 site is low as shown in Figs. 28 and 29. Low Fe_2O_3 content of these orthopyroxenes indicate that Al_2O_3 is incorporated in orthopyroxene mainly by the substitution MgSi = AlAl, whereas the substitution MgSi = Fe^{3+}Al is not so significant.

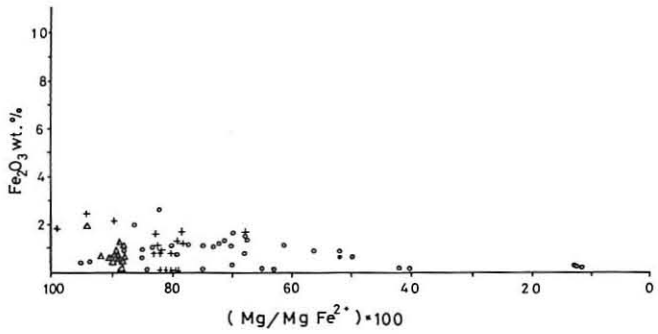

Fig. 26 The relationship between $Mg/Mg+Fe^{2+}$ and Fe_2O_3 contents of igneous orthopyroxenes. Symbols and data sources are given in Fig. 1.

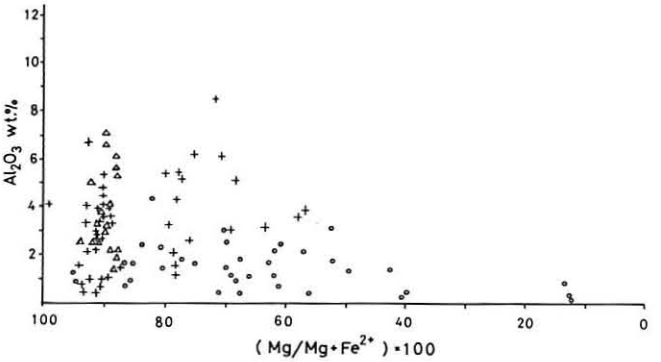

Fig. 27 The relationship between $Mg/Mg+Fe^{2+}$ and Al_2O_3 contents of igneous orthopyroxenes. Symbols and data sources are given in Fig. 1.

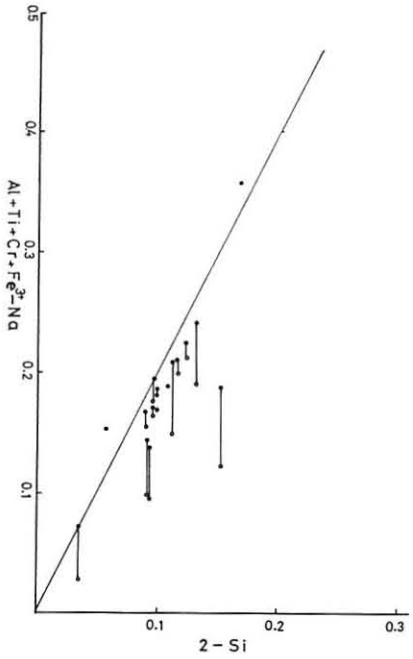

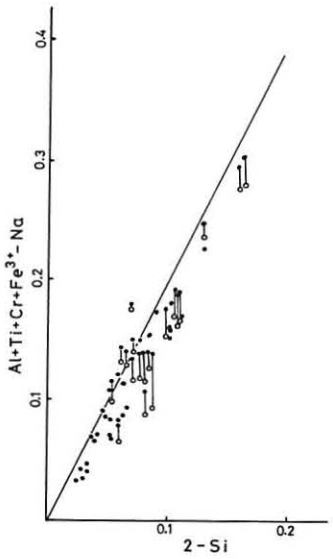

Fig. 28 (left) The relationship between (2-Si) in the tetrahedral site and (Al+Cr+Ti+Fe^{3+}-Na) in the octahedral site of orthopyroxenes from inclusions within volcanic rocks. Calculation is based on 6 oxygens. Of the two circles connected by a line, the composition of the open circle is calculated without considering Fe^{3+}. Sources of data are given in Fig. 1.

Fig. 29 (right) The relationship between (2-Si) in the tetrahedral site and (Al+Cr+Ti+Fe^{3+}-Na) in the octahedral site of orthpyroxenes from intrusive peridotites. Calculation is based on 6 oxygens. Of the two circles connected by a line, the composition of the open circle is calculated without considering Fe^{3+}. Sources of data are given in Fig. 1.

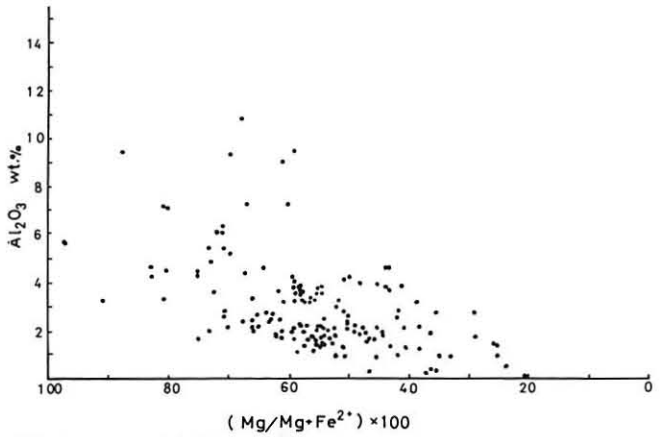

Fig. 30 The relationship between Mg/Mg+Fe^{2+} and Al_2O_3 contents of orthopyroxens from metamorphic rocks. Sources of data are given in Fig. 1.

Some orthopyroxenes from metamorphic rocks, however, show high Al_2O_3 and Fe_2O_3 contents as shown in Figs. 30 and 31. As shown in Figs. 32 and 33, the Al_2O_3 and Fe_2O_3 contents are attributed to the solubility of $MgFe^{3+}$-$AlSiO_6$ and $MgAl_2SiO_6$ in orthopyroxene. The Fe^{3+} occupies a large part of

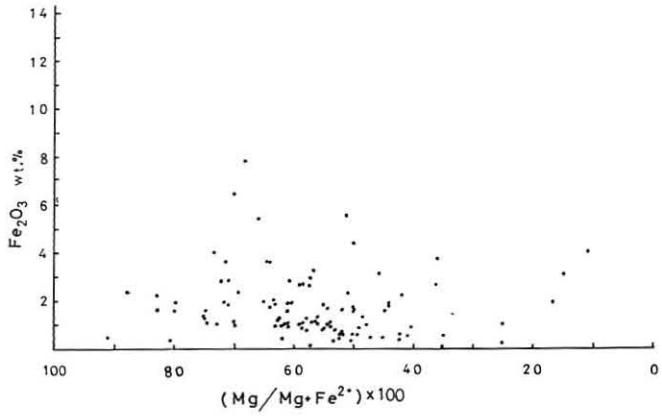

Fig. 31 The relationship between $Mg/Mg+Fe^{2+}$ and Fe_2O_3 contents of orthopyroxenes from metamorphic rocks. Sources of data are given in Fig. 1.

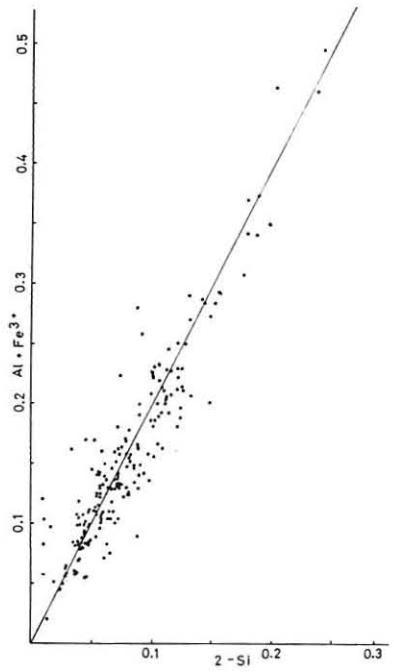

Fig. 32 The relationship between (2-Si) in the tetrahedral site and $(Al+Fe^{3+})$ in the octahedral site of orthopyroxenes from metamorphic rocks. Calculation is based on 6 oxygens. Sources of data are given in Fig. 1.

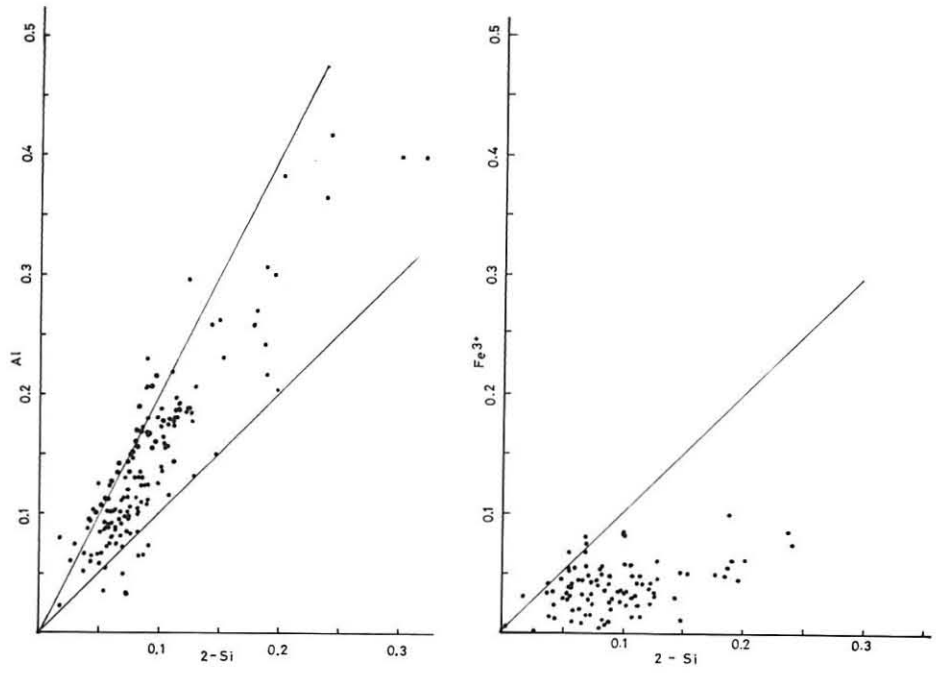

Fig. 33 (left) The relationship between (2-Si) in the tetrahedral site and (Al) in the octahedral site of orthopyroxenes from metamorphic rocks. Calculation is based on 6 oxygens. Sources of data are given in Fig. 1.

Fig. 34 (right) The relationship between (2-Si) in the tetrahedral site and (Fe^{3+}) in the octahedral site of orthopyroxenes from metamorphic rocks. Calculation is based on 6 oxygens. Sources of data are given in Fig. 1.

M1 site and there is distinct trend of increase of Fe^{3+} in M1 site with increasing silica deficiency as shown in Fig. 34. From these facts, $MgFe^{3+}AlSiO_6$ molecule is important with respect to the solubility of Al_2O_3 in orthopyroxene of some metamorphic rocks.

Present experimental results indicate that the solubility of Al_2O_3 increases with increasing Fe_2O_3 content in it at constant temperature and pressure, indicating that total Al_2O_3 content can not be used as an indicator of pressure and/or temperature. The solubility of $MgAl_2SiO_6$ in enstatite is, however, constant at constant pressure and temperature. When Al_2O_3 content is used as an indicator, it is necessary to examine the Fe_2O_3 content and only the Al_2O_3 in the $MgAl_2SiO_6$ molecule can be used.

The assemblage of high aluminous orthopyroxene+sapphirine+quartz or high aluminous orthopyroxene+sapphirine+sillimanite have been reported in several localities (Hermans et al. 1976, Morse and Talley 1971, Bondarenko 1972, Dallwitz 1968). Hermans et al. (1976) described the high aluminous orthopyroxene (9.2 wt.% Al_2O_3) coexisting with sapphirine and quartz from the migmatite near Vikesåå and estimated the crystallization temperature and pressure as 900°C and 3 – 6 Kb. Though Fe_2O_3 content of this orthopyroxene was not determined, the chemical formula suggests that about 6 wt.% Al_2O_3 is incorporated in orthopyroxene by the substitution MgSi = AlAl. On the basis of the experimental results by Arima and Onuma (1977), the estimated temperature from 9.2 wt.% Al_2O_3 is about 1200 – 1250°C, while taking $MgAl_2SiO_6$ into account an estimation from 6 wt.% Al_2O_3 by the substitution MgSi = AlAl gives temperature 1000 – 1050°C.

An aluminous and high Fe_2O_3 orthopyroxene (6.29 wt.% Al_2O_3 and 3.63 wt.% Fe_2O_3) coexisting with sapphirine and sillimanite was described by Bondarenko (1972) from Anabar Massif. This orthopyroxene shows following chemical formula, $(Mg_{1.27}Fe^{2+}_{0.50}Mn_{0.01}Ca_{0.02}Fe^{3+}_{0.10}Al_{0.09})$ $(Al_{0.18}Si_{1.82})O_6$. This formula indicates that 2.1 wt.% Al_2O_3 is incorporated in orthopyroxene as a molecule $MgFe^{3+}AlSiO_6$ and 4.2 wt.% Al_2O_3 as $MgAl_2SiO_6$. On the basis of the data by Arima and Onuma (1977), the solubility of 4.2 wt.% Al_2O_3 gives the estimation of temperature and pressure about 900°C and 12 – 16 Kb.

$Mg/Mg+Fe^{2+}$ of orthopyroxene is generally lower than that of coexisting sapphirine (Bondarenko 1972, Lutts 1968, Hermans 1976). When there is small amount of FeO in orthopyroxene and sapphirine, the molar fraction of $MgFe^{3+}AlSiO_6$ and that of $MgAl_2SiO_6$ of orthopyroxene in Eqs. 5a and 5b should decrease more than that of $Mg_2Al_4SiO_{10}$ and that of $Mg_2Fe^{3+}_4SiO_{10}$ in $sapphirine_{SS}$. With increasing $Fe^{2+}SiO_3$ content in $orthopyroxene_{SS}$ coexisting with $sapphirine_{SS}$, Eqs. 5a and 5b go toward left hand side, making the increase of Al_2O_3 content of orthopyroxene. Therefore the estimation of temperature and pressure on the basis of the experimental results in the system MgO-Al_2O_3-Fe_2O_3-SiO_2 gives the maximum values, and the actual temperature and pressure of the crystallization of such high aluminous orthopyroxenes coexisting with sapphirine and quartz, or sapphirine and sillimanite would be lower than the estimated temperature and pressure.

Conclusions

From the present experimental study, the following conclusions are obtained.

1. The phase equilibria in the system $MgSiO_3$-Al_2O_3-Fe_2O_3 are determined experimentally in the temperature and pressure range 800 – 1300°C and 8 – 16 Kb. The following phase assemblages were encountered, the single phase field of $enstatite_{ss}$, $enstatite_{ss}$+hematite, $enstatite_{ss}$+$spinel_{ss}$+quartz, $enstatite_{ss}$+$sapphirine_{ss}$+quartz, $enstatite_{ss}$+$spinel_{ss}$+hematite+quartz.
2. Al_2O_3 is incorporated in enstatite by the substitution MgSi = AlAl as well as MgSi = Fe^{3+}Al. The solubility of Al_2O_3 increases with increasing Fe_2O_3 in enstatite at constant emperature and pressure.
3. The solubility of $MgAl_2SiO_6$ in enstatite is constant at constant temperature and pressure when $enstatite_{ss}$ coexists with sapphirine and quartz.
4. The solubility of $MgFe^{3+}AlSiO_6$ in ensatite coexisting with hematite increases with increasing temperature and decreasing pressure.
5. The Al_2O_3 content of orthopyroxene can not be used as an indicator of temperature and/or pressure without taking the Fe_2O_3 content into account.

Acknowlegements

This paper is dedicated to Prof. Kenzo Yagi on the occasion of his retirement from the chair. Under his guidance I became familliar with experimental methods of silicate system and was inspired to study experimental petrology. I wish to express my sincere gratitude for his guidance and encouragement during the study.

I am grateful to the following persons. Dr. Y. Hariya and Dr. K. Onuma of Hokkaido University for their helpful discussion, Mr. S. Terada of Hokkaido University for his technical assistance on high pressure experiments, Mr. H. Ohashi of National Institute for Researches in Inorganic Material for his suggestion on high pressure experiments, Prof. I. Shinno of Kyushu University and Dr. K. Yoshikawa of Institute of Physical and Chemical Research for their discussions and performances of Mössbauer spectra.

References

Akella, J., 1976. Garnet pyroxene equilibria in the system $CaSiO_3$-$MgSiO_3$-Al_2O_3 and in a natural mineral mixture. *Amer. Miner.*, 61: 589-602.

Anastasiou, P. and Seifert, F., 1972. Solid solubility of Al_2O_3 in enstatite at high temperature and 1 – 5 kbar water pressure. *Contr. Miner. Petrol.*, 34: 272-287.

Arima, M. and Onuma, K., 1977. The solubility of alumina in enstatite and the phase equilibria in the system $MgSiO_3$-$MgAl_2SiO_6$ at 10 – 25 Kbar. *Contr. Miner. Petrol.*, 61: 251-265.

Bancroft, G.M. and Maddock, A.G., 1967. Applications of Mössbauer effect to silicate mineralogy I. Iron silicates of known crystal structure. *Geoch. Cosmoch. Acta,* 31: 2219-2246.

Bancroft, G.M. and Maddock, A.G., 1968. Applications of Mössbauer effect to silicate mineralogy II. Iron silicates of unknown and complex crystal structures. *Geoch. Cosmoch. Acta,* 32: 547-559.

Biggar, G.M. and Clark, D.B., 1973. Protoenstatite solid solution in the system CaO-MgO-Al_2O_3-SiO_2. *Lithos,* 5: 125-129.

Bondarenko, L.P., 1972. Hypersthene-kyanite association in garnet-sapphirine granulites; Thermodynamic conditions of their formation. *Internat. Geology Rev.,* 5: 466-472.

Boyd, F.R., 1973. A pyroxene geotherm. *Geochim. Cosmoch. Acta,* 37: 2533-2546.

Boyd, F.R. and England, J.L., 1959. Pyrope. *Carnegie Inst. Wash. Yearbook,* 58: 83-87.

Boyd, F.R. and England, J.L., 1964. The system enstatite-pyrope. *Carnegie Inst. Wash. Yearbook,* 63: 157-161.

Chatterjee, N.D. and Schreyer, W., 1972. The reaction $enstatite_{ss}$+sillimanite = $sapphirine_{ss}$+quartz in the system MgO-Al_2O_3-SiO_2. *Contr. Miner. Petrol.,* 36: 49-62.

Dallwitz, W.B., 1968. Co-existing sapphirine and quartz in granulite from Enderby Land, Antarctica. *Nature,* 291: 476-477.

Fujii, T. and Takahashi, E., 1976. On the solubility of alumina in orthopyroxene coexisting with olivine and spinel in the system MgO-Al_2O_3-SiO_2. *Miner. J. (Japan),* 8: 122-128.

Green, D.H. and Ringwood, A.E., 1967. The stability field of aluminous pyroxene peridotite and garnet peridotite and their relevance in upper mantle structure. *Earth Plan. Sci. Lett.,* 3: 151-160.

Hariya, Y., Dollase, W.A. and Kennedy, G.C., 1969. An experimental investigation of the relationship of mullite to sillimanite. *Amer. Miner.,* 54: 1419-1441.

Hermans, G.A.E.M., Hakstege, A.L., Jansen, J.B.H. and Poorter, R.P.E., 1976. Sapphrine occurrence near Vikeså in Rogaland, Southwestern Norway. *Norsk Geologisk Tidsskrift,* 56: 397-412.

Holdaway, M.J., 1976. Mutual compatibility relations of Fe^{2+}-Mg-Al silicates at 800°C and 3 Kb. *Amer. J. Sci.,* 276: 285-308.

Lutts, B.G. and Kopaneva, L.N., 1968. A pyrope sapphirine rock from the Anabar Massif and its conditions of metamorphism. *Earth Sci. Sect.,* 179: 161-163.

MacGregor, I.D., 1974. The system MgO-Al_2O_3-SiO_2: Solubility of Al_2O_3 im enstatite for spinel and garnet peridotite composition. *Amer. Miner.,* 50: 110-119.

MacGregor, I.D. and Ringwood, A.E., 1964. The natural system enstatite-pyrope. *Carnegie Inst. Wash. Yearbook,* 63: 161-163.

Morse, S.A. and Talley, J.H., 1971. Sapphirine reactions in deepseated granulites near Wilson Lake, Central Labrador, Canada. *Earth Planet. Sci. Lett.,* 10: 325-328.

Newton, R.C., 1972. An experimental determination of the high pressure stability limits of magnesian cordierite under wet and dry conditions. *J. Geology,* 80: 389-420.

Obata, M., 1976. The solubility of Al_2O_3 in orthopyroxenes in spinel and plagioclase peridotites and spinel pyroxenite. *Amer. Miner.,* 61: 804-816.

Ohashi, H. and Hariya, Y., 1973. Order-disorder of ferric iron and aluminum in Ca-rich clinopyroxene. *Proc. Japan Academy,* 46: 684-687.

Onuma, K. and Arima, M., 1975. The join $MgSiO_3$-$MgAl_2SiO_6$ and the solubility of Al_2O_3 in enstatite at atomspheric pressure. *J. Japan Assoc. Miner. Petrol. Econ. Geol.,* 70: 53-60.

Sakurai, T., 1968. Universal crystallographic computation program system. *Crystallogr. Japan.*

Sharma, K.K., Langer, K. and Seifert, F., 1973. Some properties of spinel phases in the binary system $MgAl_2O_4$-$MgFe_2O_4$. *N. Jb. Miner. Mh.* : 442-449.

Shinno, I., 1972. Mössbauer spectra of Fe^{3+}-pyroxene. *J. Miner. Soc. Japan,* 10: 449-458.
Skinner, B.J. and Boyd, F.R., 1964. Aluminous enstatite. *Carnegie Inst. Wash. Yearbook,* 63: 163-165.
Takeda, H., 1972. Crystallographic studies of coexisting aluminum orthopyroxene and augite of high pressure origin. *J. Geophy. Research,* 77: 5798-5811.
Virgo, D. and Hafner, S.S., 1969. Fe^{2+}, Mg order-disorder in heated orthopyroxenes. *Miner. Soc. Amer. Spec. Pap.,* 2: 67-81.
White, W.B., 1971. Direct control of oxigen vapor phase mainly at pressure greater than one atmosphere. In Ulmer, G.C.(Ed.). *Research techniques for high pressure and high temperature.* pp101-121.
Wood, B.J., 1974. The solubility of alumina in orthopyroxene coexisting with garnet. *Contr. Miner. Petrol.,* 46: 1-15.

(Received on Oct. 31, 1977)